Physical modeling of compaction with vibrating rollers in unsaturated soils

Carlos Torres*,1 and Bernardo Caicedo1

1*Department of Civil and Environmental Engineering, Los Andes University, Bogotá, Colombia*
**Corresponding author's email:* ce.torresr12@uniandes.edu.co

Abstract: Soil compaction is a necessary activity in all civil works and the soils subjected to this process are necessarily unsaturated. Today, great strides have been made in modernizing the field compaction process with the advent of continuous compaction control and intelligent compaction; however, the mechanical framework for understanding compacted soil behavior remains the Proctor test. The mechanical behavior of unsaturated compacted soils has been widely studied, and it is known that this process gives the soil an anisotropic character and the partial saturation condition exerts a strong influence on the development of plastic strains and soil densification. The study of the evolution of water content and suction in the field during vibratory compaction is difficult, so numerical modeling and recently physical modeling are used to understand how these variables influence the mechanical behavior of the soil. This article presents the results of compaction tests with a scale vibrating roller, where the evolution of suction at different depths and its influence on the development of plastic strains in the soil are studied.

Introduction

The soil compaction has been applied in construction and soil improvement since the beginning of great civilizations such as in Asia, Europe and Mesoamerica ([1]; [2]). The soils subject to this improvement process are necessarily unsaturated and the compaction paths generate anisotropic condition that, as demonstrated by [3], [4], [5] and more recently [6], influence the development of plastic strains and the increase in density. Currently, there are important advances in the modernization of the compaction process in the field, such as continuous compaction control (CCC), intelligent compaction (IC) and autonomous compaction; However, there are few investigations with an experimental approach that study the influence of suction on the development of volumetric strains, the most recent being the work of [7] where the static indentation of a pneumatic roller in the geotechnical centrifuge is studied. For this reason, the results of the study of compaction with a small-scale vibratory roller of four unsaturated soils are presented, where the response of the vibratory equipment is analyzed in terms of the force and displacement, the increase in density with depth and the changes in water content and suction during compaction.

Miniature vibrating roller compactor

The equipment used for soil compaction is presented in Figure 1 and corresponds to a 1:15 scale vibratory compactor, developed at the Universidad de los Andes in Colombia. The vibration system is based on an APA120ML piezoelectric actuator that lifts a moving mass of up to 1.0kg and allows it to apply a force of up to 400N to the soil at a frequency of 500Hz. The instrumentation is based on two accelerometers (one to determine the force and the other the displacement), a PCB208C load cell, and an Eddy current magnetic sensor was used to calibrate the displacements.

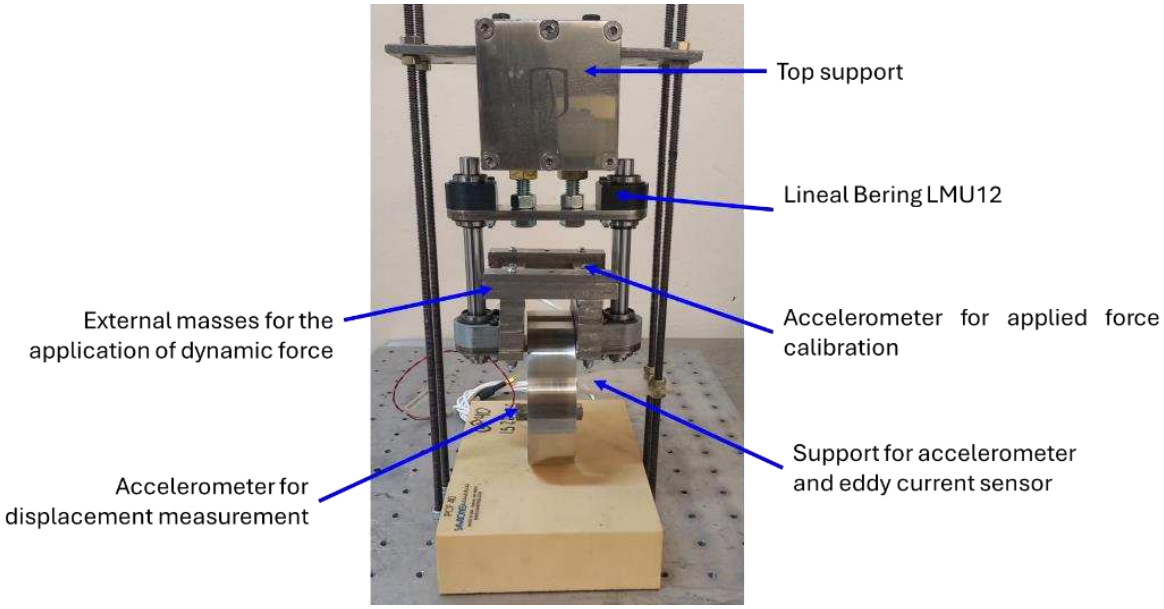

Figure 1: Miniature roller compactor used in the research

Experimental setup

The experimental procedure consisted of preparing four kaolin samples at different water contents and initial densities (Table 1). Subsequently, each sample was subjected to compaction with the vibratory roller as observed in Figure 2, applying a force with a vibration frequency of 500 Hz and duration of 20 seconds in all cases. At the end of each stage, representative samples were taken, and the water content and final suction were measured with the WP4 dewpoint potentiometer. Additionally, during each test, high-resolution videos were taken, and a particle velocimetry analysis (PIV) was performed to determine the final deformations of the soil and compare them with the theoretical model proposed by [8].

Table 1: Initial parameters of the tests

Test	wo (%)	ρ_{do} (g/cm3)	eo
T1	23.0	1.08	1.41
T2	26.0	1.01	1.84
T3	24.4	0.96	1.72
T4	36.5	1.18	1.21

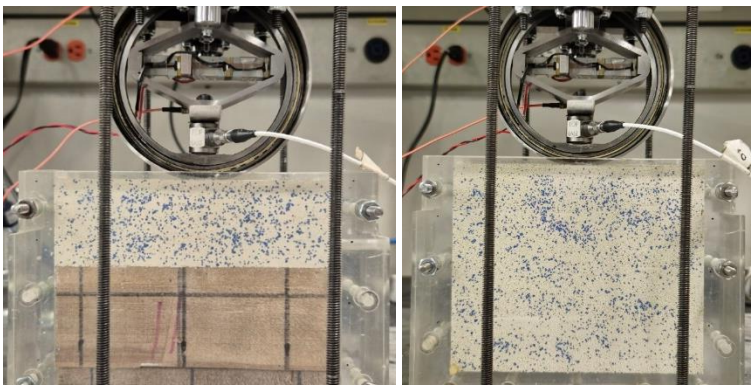

Figure 2: Detail of the setup of the two types of tests performed. Left, sample height 41mm. Right, sample height 112mm.

The compaction curve presented in Figure 3 was obtained by [9] for the same material used in the tests. The initial values of the four tests are in Figure 3. In any case, the densities were intended to be lower than the maximum to densify the material as the roller passed.

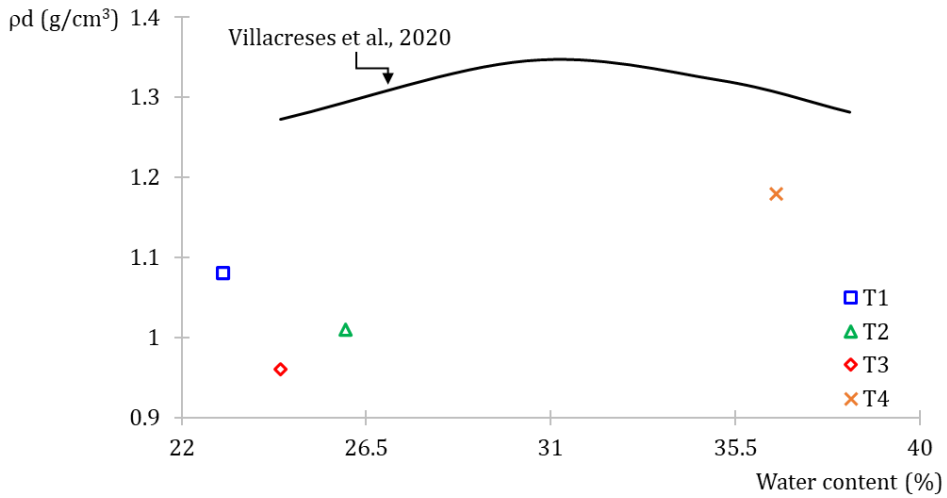

Figure 3: Initial states of testing in Proctor space

Results

Compaction

Using the accelerometer located at the bottom of the equipment, it was possible to determine the displacements, and using the load cell, it was possible to obtain the force applied in each test. Two passes of the equipment over the ground were made to see the effect of the stiffening of the ground. In Figure 4, the displacements against time and the graph of force versus displacement are presented, where it is observed that with the second pass of the compactor the soil hardens, which is evidenced by the increase in the slope of the force vs. displacement curve, and which corresponds to the secant soil stiffness (ks), it was implemented in 1999 by the Swiss company Ammann to measure changes in soil stiffness during compaction [10].

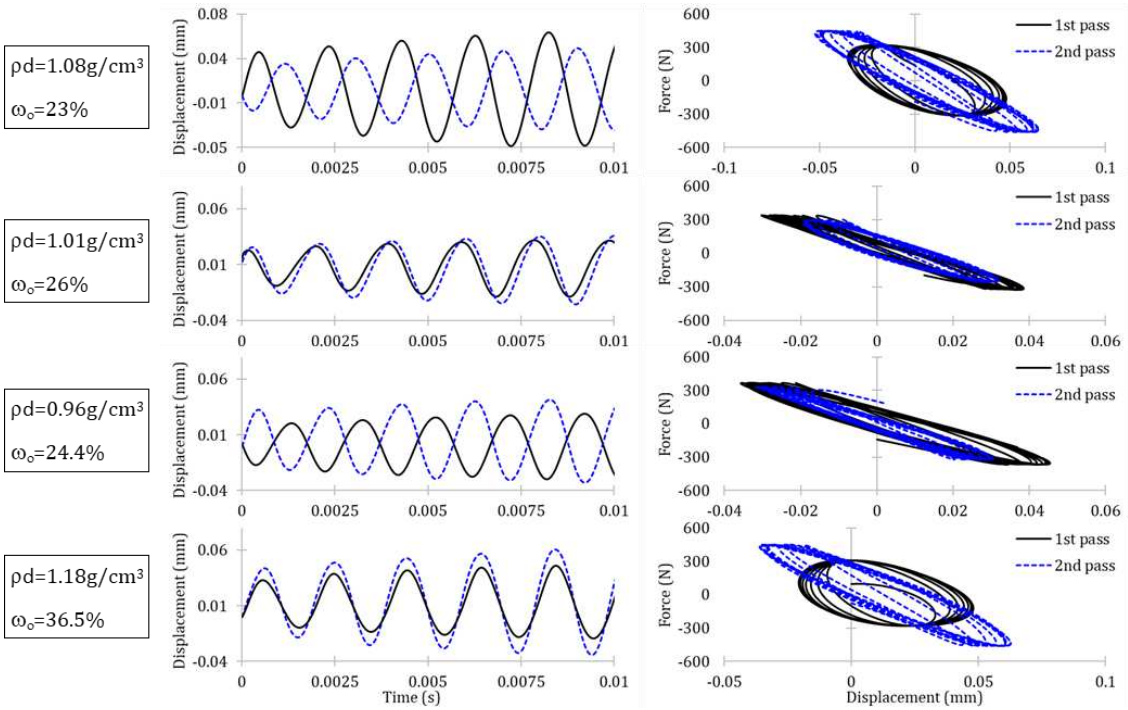

Figure 4: Results of force-displacement behavior during compaction

From the frequency content of vibration (A_Ω), the continuous compaction control coefficients CMV (compaction meter value), CCV (compaction control value) and RMV (resonant meter value) can be determined, which are described in equation (1), (2) and (3), and whose results are presented in Figure 5, where it is observed that for the highest initial densities T1 and T4, lower coefficients are obtained in the first pass, compared to the lowest densities T2 and T3. For the second pass, an increase in the coefficients is observed in densities T1 and T4; however, for densities T2 and T3 a decrease occurs, which may be due to the new density state in which these samples are found and that they are closer to the optimal water content.

$$CMV = 300\,\frac{A_{2\Omega}}{A_{\Omega}} \tag{1}$$

$$CCV = 100 \cdot \frac{A_{0.5\Omega} + A_{1.5\Omega} + A_{2.0\Omega} + A_{2.5\Omega} + A_{3.0\Omega}}{A_{0.5\Omega} + A_{\Omega}} \tag{2}$$

$$RMV = 300\,\frac{A_{0.5\Omega}}{A_{\Omega}} \tag{3}$$

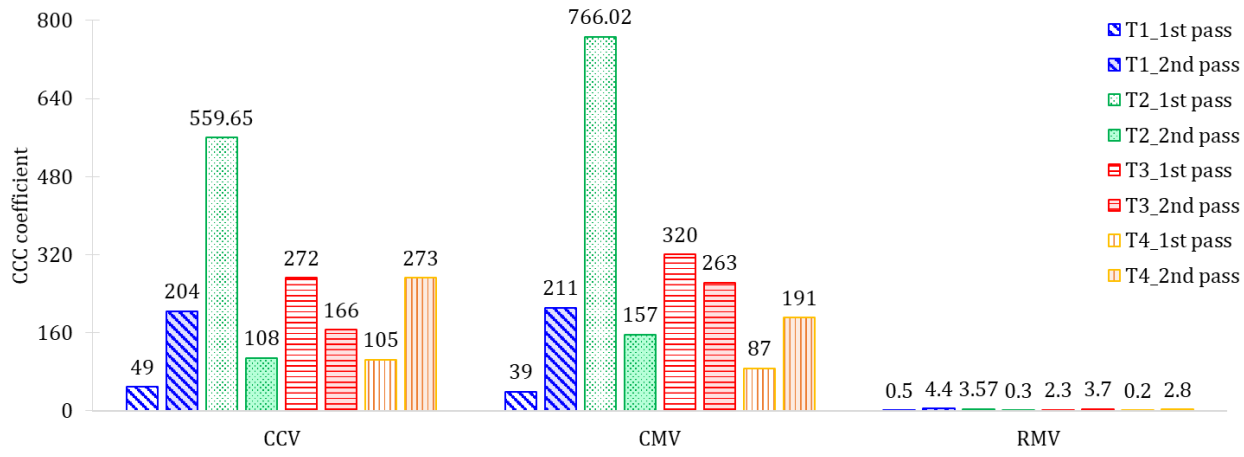

Figure 5: Variation of the CCC coefficients for the two passes of the compactor

It was also possible to obtain soil stiffness during compaction using the equation (4) of the secant soil stiffness (ks), but since this value is the slope of the force vs displacement curve, it can be obtained through an iterative process from the Hertz and Lundberg equations, the vibration module Evib. The results of this analysis shows a relationship between the initial density, the water content and the stiffness, since after compaction the modules present an increase up to the optimum water content and then decrease, presenting the same form of the compaction curve proposed by [11] as observed in Figure 6.

$$k_s = \frac{E_{vib} L \pi}{2(1-\nu^2)\left[1.8864 + \ln\left(\frac{\pi L^3 E_{vib}}{16R(1-\nu^2)F_s}\right)^{0.5}\right]} \tag{4}$$

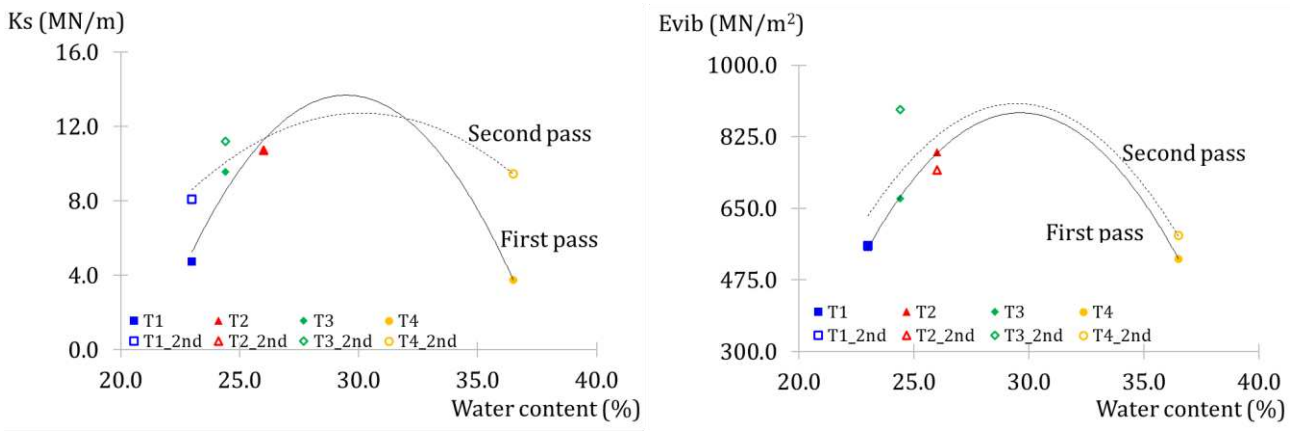

Figure 6: Relationship between the stiffness obtained during compaction and the water content in the Proctor space

PIV analysis

During all tests, high-resolution videos were taken and particle velocimeter analysis (PIV) was used to determine the deformations in the soil. In Figure 7, the settlements measured on the ground surface for the four tests performed are presented, observing that the materials with a higher initial density T1 and T4, registered low settlements, while samples T2 and T3 prepared at lower initial densities, registered greater settlements, with sample T2 being the one that presented the greatest deformation because it was closer to the optimal compaction water content.

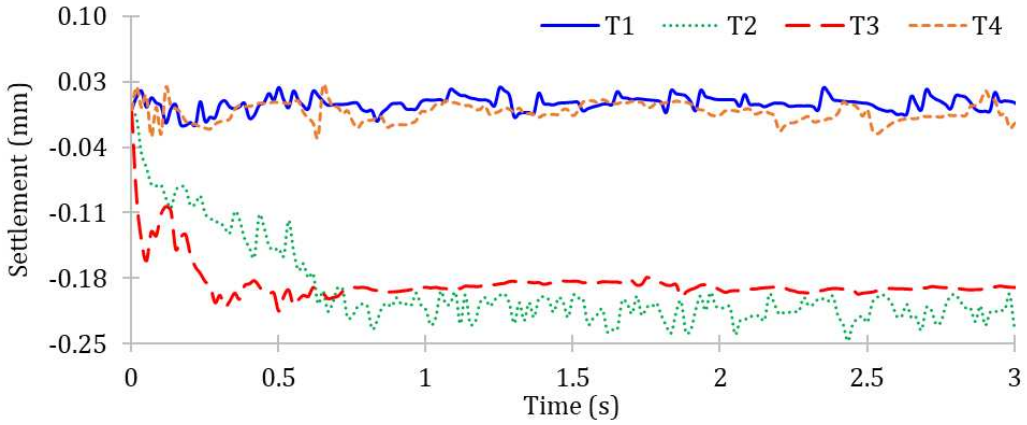

Figure 7: Settlements measured by PIV during compaction

From the PIV analysis, the divergence of the particle velocities was obtained, which is directly related to the volumetric strain rate, and from this value the deformation for each recorded frame could be obtained, the change in the void ratio and the dry density with respect to the depth, which is presented in Figure 9. As an element of comparison, the variation of the dry

density with depth was determined using the model proposed by [8], which proposes calculating the contact stresses using Hertz's theory, the increases in stresses from Fröhlich's theory and the deformations using Barcelona Basic model proposed by [12]. This model was validated by [7] from centrifuge compaction tests, obtaining a good fit in the determination of surface settlements and changes in suction during compaction.

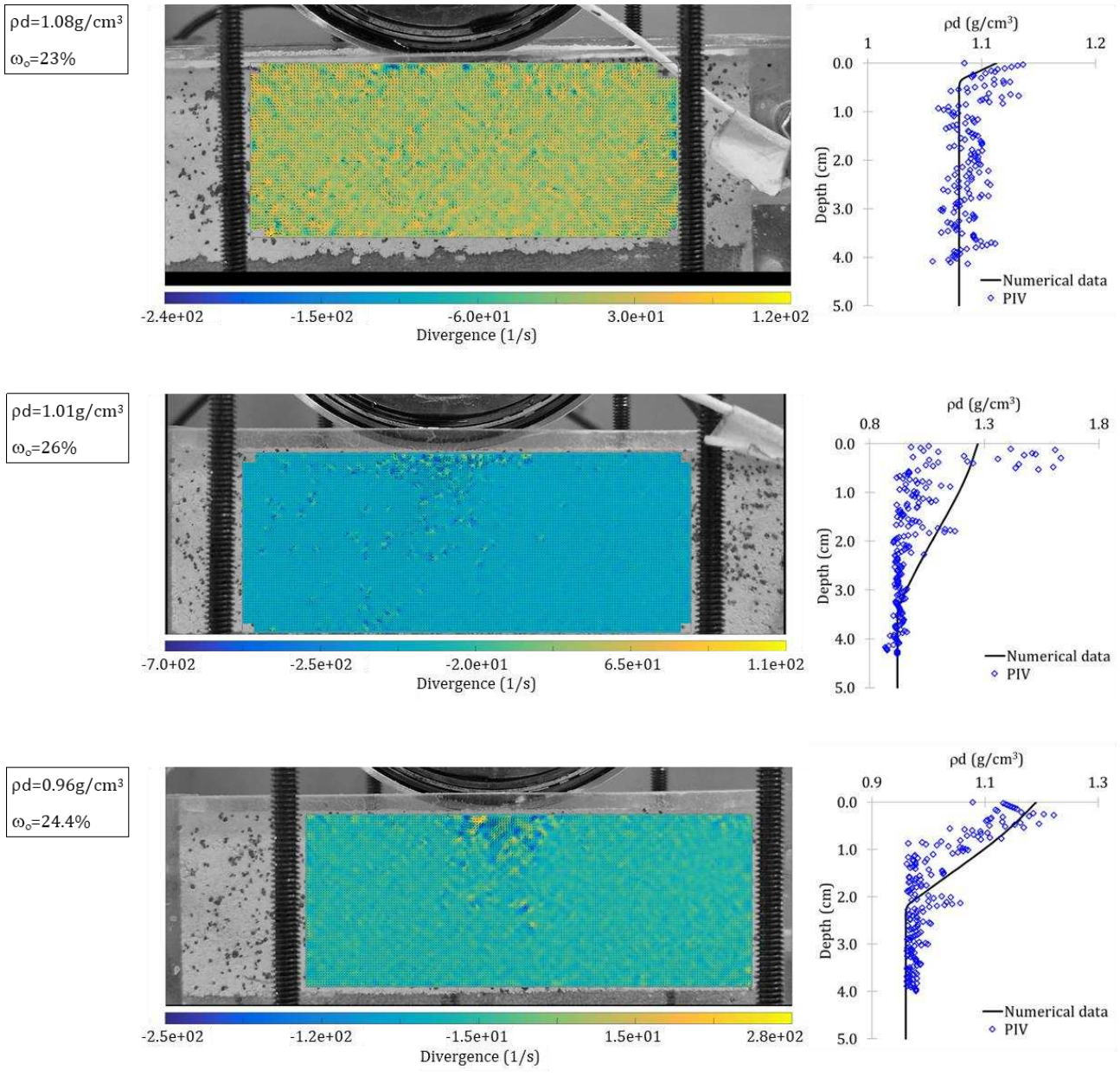

Figure 8: Dry density variation with depth for PIV analysis for the tests T1 to T3. Left, results of velocity divergence using PIV. Right, dry density obtained with PIV compared with that obtained using the numerical model.

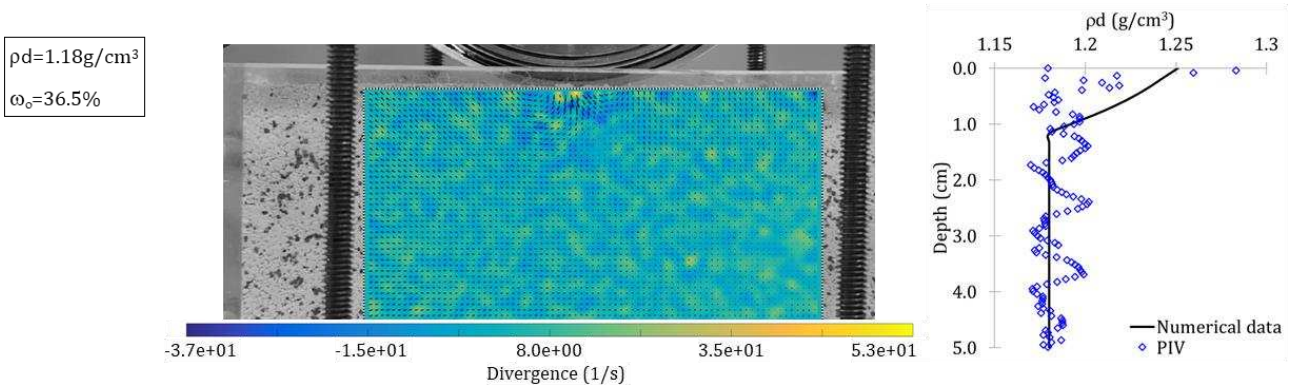

Figure 9: Dry density variation with depth for PIV analysis for the test T1. Left, results of velocity divergence using PIV. Right, dry density obtained with PIV compared with that obtained using the numerical model.

A good fit was obtained between the experimental results obtained by PIV analysis and those found by applying the [8] model, thus allowing the dry density to be determined at the end of compaction, which is presented in Figure 10, where it is observed that the samples with higher densities registered the smallest changes during compaction, compared to samples T2 and T3 which had lower initial densities and water contents closer to the optimum.

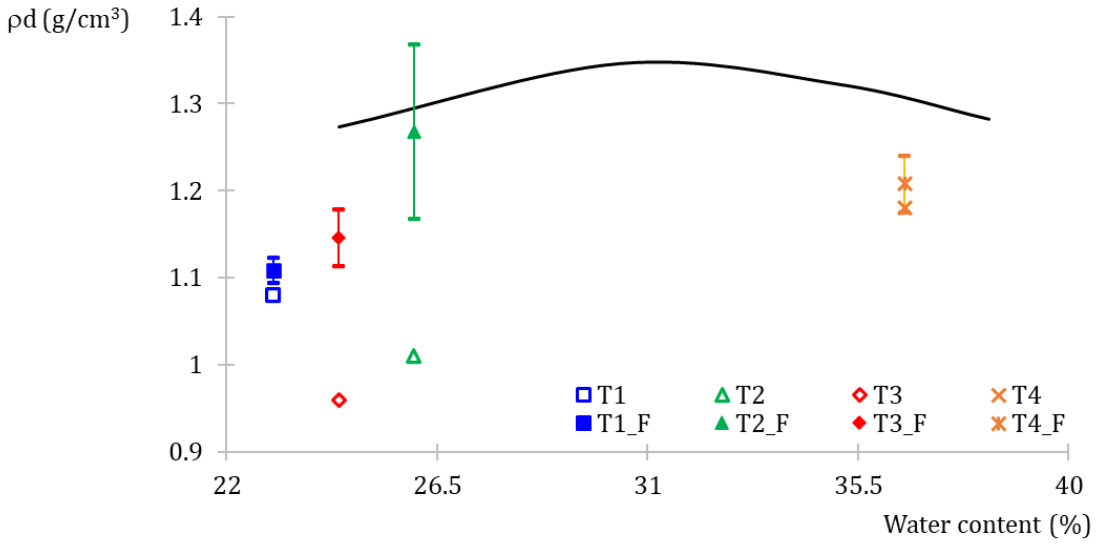

Figure 10: Initial and final states after compaction of the four tests performed

Water content and suction

At the end of each test, the water contents and total suction were determined with the WP4 dewpoint potentiometer, from 8mm diameter cylindrical samples extracted with a very thin-walled tube. In all cases, a decrease in water content was observed at a depth of 10 mm below

the surface, and then an increase in the center of the test sample, to then decrease again as observed in Figure 11. This behavior is due to the drying path that the soil showed on the surface and at the bottom during the test and the extraction of the samples. In sample T4, which had a height of 112 mm, it was observed that the water content decreases on the surface due to drying but tends to equilibrate towards the initial value at depth.

As for suction, drying profiles were also observed in which suction increased at the surface in all cases and decreased towards the depth of the samples, as observed in Figure 11. Again, sample T4, which had a greater height, registered a different behavior in suction, with an initial decrease observed near the surface and then an increase until it approached the initial suction value, a behavior like that expected during compaction and which was obtained by applying the model proposed by [8] and presented in Figure 12.

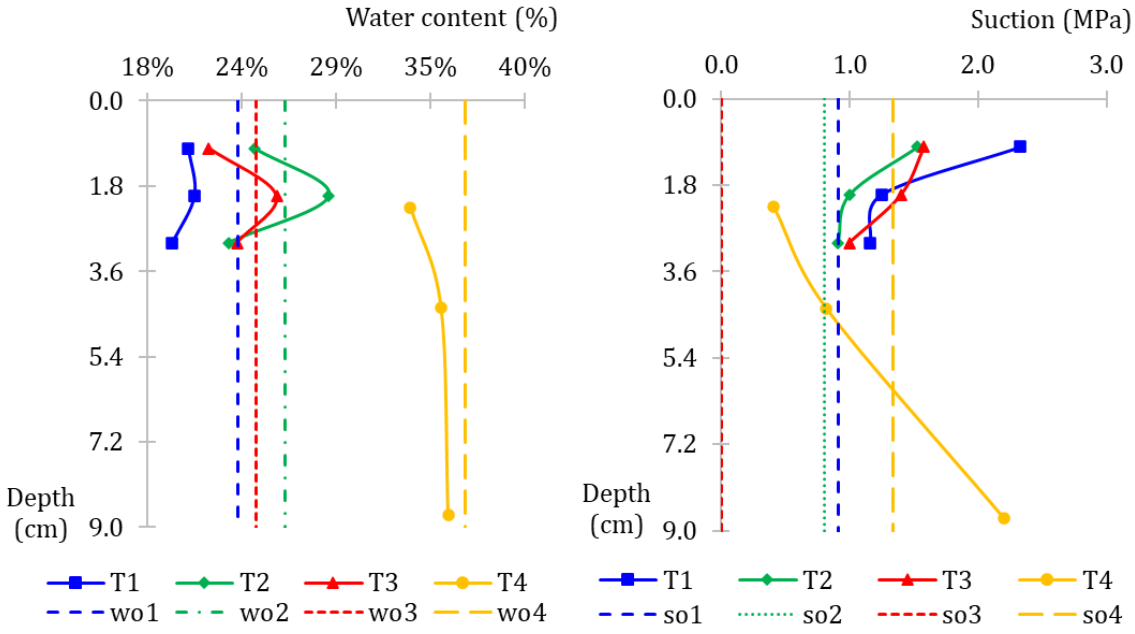

Figure 11: Evolution of water content and suction with depth after compaction. The vertical lines correspond to the initial states

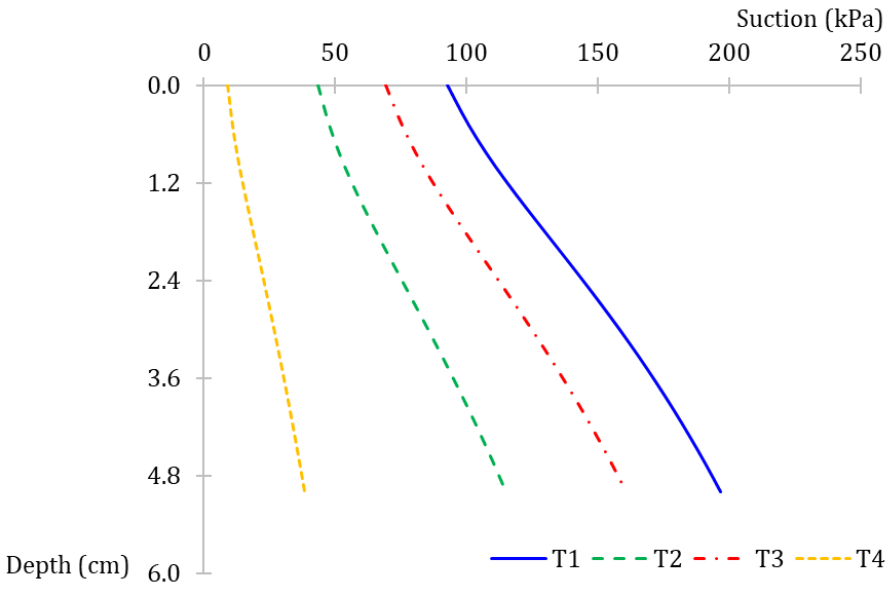

Figure 12: Suction variation with depth from the model proposed by [8]

Conclusions

The miniature compaction equipment can reproduce the behavior of a full-scale compactor roller, which was observed with the coherence between the results of the image analysis and the theoretical model for determining the density advance with depth. The instrumentation installed in the equipment allows obtaining force and displacement during compaction, with which a relationship can be obtained between the compaction trajectories in the Proctor curve space and the CCC continuous compaction control coefficients.

From the PIV image analysis, the change in density could be obtained for the two passes of the compactor that were made in each case, and it was observed how densities close to those of the Proctor compaction curve were reached, which confirms the capacity of the equipment to reproduce the compaction process on a full scale.

The analysis of changes in moisture and suction was influenced by drying during compaction and sample extraction, so it is important to refine the method for measuring the change in these parameters for the different stages of the compaction process with vibratory rollers.

References

[1] . Lay, . Metcalf and . Sharp, Paving Our Ways: A History of the World's Roads and Pavements., Reino Unido: CRC Press., 2020.

[2] . Rico Rodríguez and . Castillo, La ingeniería de suelos en las vías terrestres: carreteras, ferrocarriles y aeropistas, México: Limusa, 1981.

[3] Y. J. Cui and P. Delage, "Yielding and plastic behaviour of an unsaturated compacted silt," *Géotechnique, 46(2),* pp. 291-311, 1996.

[4] S. Leroueil and P. Barbosa, "Combined effect of fabric, bonding and partial saturation on yielding of soils," in *Rahardjo, Toll, Leong (Eds.), Unsaturated Soils for Asia*, 2000.

[5] S. Ghorbel and S. Leroueil, "An elasto-plastic model for unsaturated soils.," *Unsaturated Soils 2006 ,* pp. 1908-1919, 2006.

[6] B. Caicedo, J. Tristancho, L. Thorel and S. Leroueil, "Experimental and analytical framework for modelling soil compaction.," *Engineering geology, 175,* pp. 22-34, 2014.

[7] A. Escobar, B. Caicedo and M. Cabrera, " Interaction between a cylinder and a partially saturated soil for compaction analysis.," *Transportation Geotechnics, 30, 100600.,* 2021.

[8] B. Caicedo, "Mechanical Framework for Modelling Soil Compaction," in *PanAm Unsaturated Soils*, 2017.

[9] J. Villacreses, B. Caicedo, S. Caro and F. Yépez, "A novel procedure to determine shear dynamic modulus and damping ratio for partial saturated compacted fine-grained soils," *Soil Dynamics and Earthquake Engineering,* 2020.

[10] S. Nazarian, A. Fathi, C. Tirado, V. Kreinovich, S. Rocha and M. Mazari, Evaluating mechanical properties of earth material during intelligent compaction, NCHRP RESEARCH REPORT 933, 2020.

[11] R. Proctor, "Description of Field and Laboratory Methods," *Engineering news record 111,* pp. 289-293, 1933 (b).

[12] E. E. Alonso, A. Gens and A. Josa, "A constitutive model for partially saturated soils.," *Géotechnique, 40(3),* pp. 405-430, 1990.